

SUPPLEMENTAL MATERIAL

- A. Detailed Materials and Methods
- B. Supplemental References
- C. Online Tables
 - Online Table I. gRNA sequences for CRISPR/Cas9
 - Online Table II. Primers
 - Online Table III. Antibody and Dye List
- D. Online Figures
 - Online Figure I. AAV ITR vector for delivery of tandem guide RNAs and cTNT-Cre
 - Online Figure II. Distribution of GFP and tdTomato reporters in Rosa26^{Cas9GFP/tdTomato} mice after treatment with AAV9:TNT-Cre
 - Online Figure III. Frame-shift mutations induced by Jph2gRNA-directed Cas9 cleavage followed by NHEJ
 - Online Figure IV. JPH2 immunoblot of FACS-sorted GFP+ CMs treated with TNT-Cre or Jph2(gRNA1+2) AAV.
 - Online Figure V. JPH2 depletion did not cell-autonomously disrupt sarcomere organization
 - Online Figure VI. Depletion of NKX2-5, TEAD1 and CAV3 by CASA AV
 - Online Figure VII. Mosaic RYR2 depletion using multiple gRNA pairs disrupts T-tubule structure.
- E. Online Movies
 - Online Movie I. *In situ* T-tubule imaging in a Jph2_Low heart
 - Online Movie II. *In situ* T-tubule imaging in a Jph2_Mid heart
 - Online Movie III. *In situ* T-tubule imaging in a Jph2_High heart
 - Online Movie IV. *In situ* T-tubule imaging in a RYR2 mosaic mutagenesis heart

A. Detailed Materials and Methods

Plasmid construction

AAV-U6-TnT-Cre ITR plasmid was developed by modification of PX552 (Addgene #60958). PX552 was digested with XbaI and HindIII to remove the hSyn promoter and eGFP cDNA. A 414 bp chicken cardiac Troponin T promoter + β Globin intron and Cre cDNA was PCR amplified with primers tagged with SpeI 5' and HindIII 3' from an AAV-TnT-Cre plasmid reported previously¹. The TnT-Cre amplicon was then cloned into the digested PX552 vector. Addition of a second U6 promoter and gRNA scaffold was achieved by cloning the second U6 promoter and a 5' AarI site into the MluI site upstream of the first U6 promoter. An additional AarI site and the second gRNA scaffold was then cloned into the same MluI site. See Online Fig. I for the map of gRNA cloning strategy this plasmid. gRNAs (Online Table I) were designed using an online tool (<http://crispr.mit.edu/>) and cloned into the first or second U6 promoter cloning sites.

AAV9 production

AAV9 was prepared using standard protocols² with modifications. In brief, AAV-ITR plasmids, AAV9-Rep-Cap, and pHelper (pAd-deltaF6, Penn Vector Core) plasmids were produced by maxiprep (Invitrogen, K210017). Triple transfection into AAV293 cells (Agilent, 240073) was performed using PEI transfection reagent (Polysciences, 23966-2). 60h after transfection, cells were scraped off of plates, resuspended in lysis buffer (20 mM Tris pH 8, 150 mM NaCl, 1 mM MgCl₂, 50 μ g/ml Benzonase) and lysed by three freeze-thaw cycles. AAV9 was precipitated by PEG8000 (VWR, 97061-100) and re-suspended in lysis buffer. AAV was purified in a density gradient (Cosmo Bio USA, AXS-1114542) by ultracentrifugation (Beckman, XL-90) with a VTi-50 rotor and concentrated in PBS using a 100 kD filter tube (Fisher Scientific, UFC910024). AAV titer was quantified by Q-PCR (primer sequences in Online Table II) using a fragment of the TNT promoter DNA to make a standard curve.

Animal experiments

All animal procedures were approved by the Institutional Animal Care and Use Committee of Boston Children's Hospital. Rosa^{Cas9GFP/Cas9GFP} and Rosa^{tdTomato/tdTomato} mice were acquired from the Jackson Laboratory.

To inject AAV into P1 pups, the body weight of the animals was measured and the pups were anesthetized in an isoflurane chamber. The amount of AAV was calculated according to body weight and injected subcutaneously.

Echocardiography was performed on a VisualSonics Vevo 2100 with Vevostrain software. Animals were awake during this procedure and held in a standard handgrip. Echocardiography was performed blinded to treatment group.

Gene expression analysis

Total RNA was purified from the heart apex using PureLink RNA Mini kit (Ambion, 12183025). Genomic DNA removal from RNA and reverse transcription was performed using QuantiTech reverse transcription kit (Qiagen, 205311). Real-time PCR was performed using an ABI 7500 thermocycler with Power SYBR Green PCR kit (ThermoFisher, 4368702). Primers are listed in Online Table II.

Amplicon Sequencing

Primers that were used to generate DNA libraries are listed in Online Table II. DNA library construction protocol was modified from our previous protocol³. In brief, targeted cDNA sequences were amplified by PCR using Phusion High-Fidelity DNA polymerase (NEB, M0530S). The amplicons were next phosphorylated by T4 polynucleotide kinase (NEB, M0201S) and adenylated by Klenow fragment (3'-5' exo-) (NEB, M0212S). Adaptor primers were phosphorylated, annealed and ligated to both ends of the amplicons through T-A ligation using Quick Ligation kit (NEB, M2200S). Multiplexing primers were next used to barcode and PCR amplify the DNA libraries. After each step above, DNA was purified by AMPure XP beads (Beckman, A63881) under 1.6X conditions. Then an equal amount of each library was pooled together and gel purified to remove free primers and primer dimers. 250 bp paired end sequencing was performed on a MiSeq Sequencer (Illumina).

Amplicon-Seq reads were first quality controlled and trimmed to remove adapter sequences (Multiplexing adapter 1: p-GATCGGAAGAGCACACGTCT, Multiplexing adapter 2: ACACTCTTTCCTACACGACGCTCTCCGATCT) using Trim Galore (a wrapper tool around Cutadapt⁴ and FastQC) (http://www.bioinformatics.babraham.ac.uk/projects/trim_galore/). Insertions/deletions in the trimmed sequencing libraries were then quantified using CRISPResso software⁵ run with the optional parameters -g, -c and --hide_mutations_outside_window_NHEJ. For analyzing amplicon 1&2, we ran CRISPResso in single-end mode (using read1 files) as the read length was longer than the amplicon size. However amplicon 3 is 512 bp in size and therefore we analyzed it by utilizing the paired end option (using parameter -r2 to specify read2 files).

Cardiomyocyte isolation and culture

Cardiomyocytes were isolated by Langendorff perfusion using an established protocol⁶ with modifications. In brief, heparin-injected mice were anesthetized in an isoflurane chamber. Hearts were isolated and cannulated onto the perfusion apparatus. Perfusion buffer [10 mM Hepes (pH 7.4), 120.4 mM NaCl, 14.7 mM KCl, 0.6 mM KH₂PO₄, 0.6 mM Na₂HPO₄, 1.2 mM MgSO₄, 4.6 mM NaHCO₃, 30 mM Taurine, 10 mM 2,3-butanedione monoxime, 5.5 mM glucose] was pumped into the heart to clear blood and equilibrate the organ. Retrograde perfusion of collagenase II (Worthington, LS004177) was performed in the heart for 10 min at 37 °C to dissociate

cardiomyocytes. Heart apex was cut from the digested heart, manually dissociated into single cardiomyocytes in 10% FBS/perfusion buffer, and filtered through a 100 µm cell strainer to remove undigested tissues. The isolated cardiomyocytes were concentrated by 20 x g low-speed centrifugation for 4 min and re-suspended in short-term culture medium (DMEM (Gibco), 10% FBS, pen/strep (Gibco), 10 µM Blebbistatin). Cardiomyocytes were cultured on laminin-coated coverslips in culture medium for <1 h at 37 °C with 5% CO₂ before fixation.

Flow Cytometry

For flow cytometry analysis, freshly isolated CMs were passed through a 100 µm cell strainer and centrifuged at 20 x g for 5 minutes at room temperature. Non-myocytes in the supernatant were discarded and the pelleted CMs were resuspended in 2.5 ml of PBS. Fluorescence data were collected on a Propel Laboratories Avalon cytometer with a 100 µm nozzle and standard GFP/RFP filter sets. Data were further analyzed using BioRad ProSort software.

For FACS, CMs from each heart were passed through a 100 µm cell strainer, centrifuge at 20 x g for 5min at RT, resuspended in ~1ml perfusion buffer. FACS were performed using a BD Ariall SORP cell sorter with a 100 µm nozzle. GFP+ CMs were collected in 1.5 ml Eppendorff tubes with cold perfusion buffer.

Histology analysis

After mice were euthanized by CO₂, body weight was measured using a digital benchtop scale (Sartorius, AY123). Hearts were removed, gently blotted to remove liquid, and weighed using an analytical balance (Fisher Science Education). Bright-field images of whole hearts were taken under a dissection microscope (Zeiss, SteREO Discovery V8). Images of hearts that were isolated from mice with similar body weights (<10% difference) were put together for comparison.

Hearts were fixed by 4% paraformaldehyde overnight at 4 °C and cryoprotected by washing in 15% followed by 30% sucrose. Hearts were embedded in tissue freezing medium (General Data, TFM-5). 10 µm cryo-sections were cut using a cryostat (Thermo Scientific, Microm HM 550).

Hematoxylin & eosin staining was performed on cryo-sections. Sections were first air dried at room temperature, stained with 0.1% Mayers Hematoxylin for 10 min and rinsed in water for 5 min. Next the sections were dipped in 0.5% Eosin for 2 min and rinsed in water for 2 min. Then the sections were dipped in 50%, 70%, 95%, 100% ethanol and Xylene. After air drying, the sections were mounted using VectaMount permanent mounting medium (Vector Laboratories, H5000).

Immunofluorescence

Isolated cardiomyocytes were immunostained as described previously^{7,8}. In brief, cardiomyocytes in culture were fixed on coverslips by 4% paraformaldehyde/PBS for 10

min, permeabilized by 0.1% Triton-100/PBS for 10 min, and blocked in 4% BSA/PBS at room temperature for 1 h. Then the cells were incubated with primary antibodies diluted in blocking buffer overnight at 4 °C. After three 5 min washes with blocking buffer, the cells were incubated with secondary antibodies and dyes at room temperature for 2 h. Then the cells were washed with PBS three times and mounted with ProLong Diamond antifade mountant (Invitrogen, 36961)

To immunostain tissue sections, frozen sections were first warmed to room temperature, incubated with 0.1% Triton-100/PBS for 10 min, and blocked with 4% normal donkey serum/PBS at room temperature for 2 h. Then the cells were incubated with primary antibodies diluted in blocking buffer overnight at 4 degree. After three 15 min washes with blocking buffer, the cells were incubated with secondary antibodies with/without WGA and/or DAPI at room temperature for 2 h. Then the sections were washed with PBS for 15 min/each for three times and mounted with ProLong Diamond antifade mountant (Invitrogen, 36961)

All antibodies and dyes used in this study are listed in Online Table III.

Western blot

FACS sorted CMs were lysed in 2X SDS sample buffer at 2000 cell/ul concentration to normalize protein contents. After boiled for 5 min, 5 µl cell lysate of each sample was separated on a 4%-12% gradient gel (Invitrogen, Bolt gels, NW04122BOX), transferred to a PDVF membrane, and blocked by 4% milk/TBST. Primary antibodies were incubated with the membrane overnight at 4°C, followed by four 15min TBST washes. HRP-conjugated secondary antibodies were probed for 1~2h at RT, followed by four 15 min TBST washes. After adding Immobilon Western chemiluminescent HRP substrate (Millipore, WBKLS0500), chemiluminescence were detected by a Li-Cor C-DiGit blot scanner.

All antibodies used in this study are listed in Online Table III.

In situ confocal T-tubule imaging

In situ T-tubule imaging was performed following a published protocol⁹ with modifications. In brief, hearts were dissected from euthanized animals and cannulated on a Langendorff apparatus. 100 µg/ml FM 4-64 (Invitrogen, 13320) was loaded into the heart by retrograde perfusion at room temperature for 10 min. The heart was next removed from the perfusion system, positioned on a glass-bottom dish, and immediately imaged by confocal microscopy.

Microscopy and image analysis

All bright-field images was taken under a stereomicroscope (Zeiss SteREO Discovery V8) with an AxioCam MRc camera. All confocal fluorescence images were taken using Olympus FV1000 inverted laser scanning confocal microscope equipped with an EM-CCD camera. A 60X/1.3 silicone-oil objective was used to image all

intracellular structures including t-tubule, sarcomere and nuclei. A 10X air objective was used to image whole tissue sections. Brightness and contrast were adjusted using ImageJ. All cell-counting-based quantification was performed manually under Nikon Eclipse 90i microscope with a Plan Fluor 40x/0.75 objective.

For JPH2 immunofluorescence intensity measurement on single cells, all cells were cultured, stained and imaged side-by-side under the same conditions on the same day. Cell boundary was manually drawn on maximally projected images and the average pixel intensity within the outlined images was measured using ImageJ. Background intensity was determined by measuring cell-free areas and was subtracted from the JPH2 average intensity.

Quantification of T-tubule and sarcomere were performed using AutoTT v1.0 software¹⁰.

Intracellular Ca²⁺ imaging

Intracellular Ca²⁺ recordings were performed after loading CMs with Rhod-2 AM (8 µmol/L, Molecular Probes) for 30 min. After loading, CMs were subsequently washed with normal Tyrode solution (NaCl, 140 mM; KCl, 4 mM; MgCl₂, 1 mM; CaCl₂, 1.8 mM; Glucose, 10 mM; and HEPES, 5 mM, pH = 7.4, adjusted with NaOH) to remove the excess dye for 20 min. Cells were electrically stimulated at 1 Hz to produce steady-state conditions. All image data were acquired in the line scanning mode along the long axis of the cell. Line scan was positioned in the cytosol, avoiding the nuclear area. Ca²⁺ levels were reported as F/F₀, where F₀ is the resting Ca²⁺ fluorescence. A Olympus FV1000 inverted laser scanning confocal microscope with a 60X/1.3 silicone-oil objective was used for confocal fluorescence imaging by line scan.

B. Supplemental References

1. Prendiville TW, Guo H, Lin Z, Zhou P, Stevens SM, He A, VanDusen N, et al. Novel Roles of GATA4/6 in the Postnatal Heart Identified through Temporally Controlled, Cardiomyocyte-Specific Gene Inactivation by Adeno-Associated Virus Delivery of Cre Recombinase. *PLoS One*. 2015;10:e0128105.
2. Grieger JC, Choi VW, Samulski RJ. Production and characterization of adeno-associated viral vectors. *Nat Protoc*. 2006;1:1412–1428.
3. He A, Pu WT. Genome-wide location analysis by pull down of in vivo biotinylated transcription factors. *Curr Protoc Mol Biol*. 2010;Chapter 21:Unit 21.20.
4. Martin M. Cutadapt removes adapter sequences from high-throughput sequencing reads. *EMBnet.journal*. 2011;17:10–12.
5. Pinello L, Canver MC, Hoban MD, Orkin SH, Kohn DB, Bauer DE, Yuan G-C. Analyzing CRISPR genome-editing experiments with CRISPResso. *Nat Biotechnol*. 2016;34:695–697.
6. O’Connell TD, Rodrigo MC, Simpson PC. Isolation and Culture of Adult Mouse Cardiac Myocytes. In: Vivanco F, editor. Cardiovascular Proteomics. Humana Press; p. 271–296.
7. Guo Y, Kim Y, Shimi T, Goldman RD, Zheng Y. Concentration-dependent lamin assembly and its roles in the localization of other nuclear proteins. *Mol Biol Cell*. 2014;25:1287–1297.
8. Guo Y, Zheng Y. Lamins position the nuclear pores and centrosomes by modulating dynein. *Mol Biol Cell*. 2015;26:3379–3389.
9. Chen B, Zhang C, Guo A, Song L-S. In situ single photon confocal imaging of cardiomyocyte T-tubule system from Langendorff-perfused hearts. *Front Physiol*. 2015;6:134.
10. Guo A, Song L-S. AutoTT: automated detection and analysis of T-tubule architecture in cardiomyocytes. *Biophys J*. 2014;106:2729–2736.

C. Online Tables

Online Table I. gRNA design for CRISPR/Cas9 mutagenesis

Gene target	gRNA target 1	gRNA target 2
<i>tdTomato</i>	ggcgagggccgcccctacga	n/a
<i>Jph2</i>	gatgatggcggggcgattg	attccaagtgcctcgtact
<i>Nkx2-5</i>	tggcctcgaggcgcgacagac	gaccctcgggcgataaaaa
<i>Tead1</i>	ccgattgacaacgacgcgga	tggctatctatccgccgtgt
<i>Mef2c</i>	acaacgagccgcacgagagc	ccatgtcagtgctggcgtag
<i>Tbx5</i>	tggcctggcgcgacgcctc	caagtctccatcatccccgc
<i>Ryr2</i>	cctgcagggcccgtactgac	gtgcagatagacagggtccgg
<i>Ryr2 Pair2</i>	cctgtcagtagcgggcccctgc	gcacaaagggtgcagatagac
<i>Ryr2 Pair3</i>	tgagggtggttctgcagtgca	tgcttggcagcagaaggatt
<i>Cav3</i>	gaccgaagagcacacggatc	cattgatggttcttggggtcg
<i>Cacna1c</i>	agccatcgatgccgcccggc	ttatgcacgccctccggata
<i>Ncx1</i>	tgtttcaatgggatttcgtc	ctctcgctcacgtgagtcac

Online Table II. Primers

Primers for amplicon sequencing		
	primer 1	primer 2
Amplicon 1 PCR	ctagcccgggtggtgagtcta	gtattcacctggcccttgg
Amplicon 2 PCR	gacatgggcttggcatagag	gttggtgaattggccttgat
Amplicon 3 PCR	ctagcccgggtggtgagtcta	gttggtgaattggccttgat
Adaptor primers	gatcgggaagagcacagtct	acactctttccctacacgacgctcttccgatct
universal barcoding primer	aatgatacggcgaccaccgagatctacactctttccctacacgacgctcttccgatct	
multiplexing barcoding primer (where bold indicates barcodes designed according to NEB 96-multiplexing kit, E6609)		
1	caagcagaagacggcatacagagat gtcggtaa gtgactggagttcagacgctgtgctcttccgatct	
2	caagcagaagacggcatacagagat aggctact gtgactggagttcagacgctgtgctcttccgatct	
3	caagcagaagacggcatacagagat gaatccga gtgactggagttcagacgctgtgctcttccgatct	
4	caagcagaagacggcatacagagat gtaccttg gtgactggagttcagacgctgtgctcttccgatct	
5	caagcagaagacggcatacagagat catgaggag gtgactggagttcagacgctgtgctcttccgatct	
6	caagcagaagacggcatacagagat tgactgac gtgactggagttcagacgctgtgctcttccgatct	
7	caagcagaagacggcatacagagat cgatttcgg gtgactggagttcagacgctgtgctcttccgatct	
8	caagcagaagacggcatacagagat ctcctaga gtgactggagttcagacgctgtgctcttccgatct	
9	caagcagaagacggcatacagagat tagttgcg gtgactggagttcagacgctgtgctcttccgatct	
10	caagcagaagacggcatacagagat gagatacgg gtgactggagttcagacgctgtgctcttccgatct	
11	caagcagaagacggcatacagagat agggttac gtgactggagttcagacgctgtgctcttccgatct	
12	caagcagaagacggcatacagagat taatgccc gtgactggagttcagacgctgtgctcttccgatct	
13	caagcagaagacggcatacagagat tcagacga gtgactggagttcagacgctgtgctcttccgatct	
14	caagcagaagacggcatacagagat gataggct gtgactggagttcagacgctgtgctcttccgatct	
15	caagcagaagacggcatacagagat tggtacag gtgactggagttcagacgctgtgctcttccgatct	
16	caagcagaagacggcatacagagat caaggctc gtgactggagttcagacgctgtgctcttccgatct	
17	caagcagaagacggcatacagagat gctatcct gtgactggagttcagacgctgtgctcttccgatct	
18	caagcagaagacggcatacagagat atggaagg gtgactggagttcagacgctgtgctcttccgatct	
19	caagcagaagacggcatacagagat tcaaggac gtgactggagttcagacgctgtgctcttccgatct	
20	caagcagaagacggcatacagagat gttacgca gtgactggagttcagacgctgtgctcttccgatct	
21	caagcagaagacggcatacagagat agtctgtg gtgactggagttcagacgctgtgctcttccgatct	
22	caagcagaagacggcatacagagat gcacgtaa gtgactggagttcagacgctgtgctcttccgatct	
23	caagcagaagacggcatacagagat aaccttgg gtgactggagttcagacgctgtgctcttccgatct	
24	caagcagaagacggcatacagagat attgctgtg gtgactggagttcagacgctgtgctcttccgatct	
25	caagcagaagacggcatacagagat acctgga gtgactggagttcagacgctgtgctcttccgatct	
26	caagcagaagacggcatacagagat ggagatga gtgactggagttcagacgctgtgctcttccgatct	
27	caagcagaagacggcatacagagat gtactctc gtgactggagttcagacgctgtgctcttccgatct	
28	caagcagaagacggcatacagagat gtaacgac gtgactggagttcagacgctgtgctcttccgatct	
29	caagcagaagacggcatacagagat attcctcc gtgactggagttcagacgctgtgctcttccgatct	
30	caagcagaagacggcatacagagat gtgttcct gtgactggagttcagacgctgtgctcttccgatct	
31	caagcagaagacggcatacagagat aagcactg gtgactggagttcagacgctgtgctcttccgatct	
32	caagcagaagacggcatacagagat ctagcaag gtgactggagttcagacgctgtgctcttccgatct	
33	caagcagaagacggcatacagagat tgcttcca gtgactggagttcagacgctgtgctcttccgatct	
34	caagcagaagacggcatacagagat gcttagct gtgactggagttcagacgctgtgctcttccgatct	
35	caagcagaagacggcatacagagat aaccgttc gtgactggagttcagacgctgtgctcttccgatct	
36	caagcagaagacggcatacagagat gacattcc gtgactggagttcagacgctgtgctcttccgatct	
37	caagcagaagacggcatacagagat agaccgta gtgactggagttcagacgctgtgctcttccgatct	
38	caagcagaagacggcatacagagat gatactgg gtgactggagttcagacgctgtgctcttccgatct	
39	caagcagaagacggcatacagagat tgcttaga gtgactggagttcagacgctgtgctcttccgatct	
40	caagcagaagacggcatacagagat tcggttac gtgactggagttcagacgctgtgctcttccgatct	
41	caagcagaagacggcatacagagat atgacgtc gtgactggagttcagacgctgtgctcttccgatct	
42	caagcagaagacggcatacagagat gctgtaag gtgactggagttcagacgctgtgctcttccgatct	
Primers for quantitative PCR		
Gene	Primer 1	Primer 2
<i>Jph2</i>	gtccaacatcgcccgtacatt	gccgacgcttctgatactcc
<i>Gapdh</i>	aggctcgggtgtgaacggatctt	tgtagaccatgtagttgaggtca
<i>Nppa</i>	ttcctcgtcttggcctttt	cctcatcttctaccggcatc
<i>Nppb</i>	gtccagcagagacctcaaaa	aggcagagtcagaaactgga
<i>Myh7</i>	gcgactcaaaaagaaggacttt	ggcttgctcatcctcaatcc
<i>AAV titer</i>	tcgggataaaaagcagtctgg	ccaagctattgtgtggcct

Online Table III. Antibodies and dyes used in this study

Name	Dilution (Application)	Company	Cat. No.
<i>Primary Antibodies</i>			
Rb-anti-JPH2	1:200 (IF), 1:2000 (WB)	Invitrogen	405300
Gt-anti-CAV3	1:200 (IF)	Santa Cruz	7665
Ms-anti-ACTN2	1:500 (IF)	Abcam	9465
Gt-anti-Troponin I	1:500 (IF)	Abcam	56357
Ms-anti-RYR2	1:200 (IF)	Abcam	2728
Gt-anti-NKX2-5	1:200 (IF)	Santa Cruz	8697
Ms-anti-TEAD1	1:500 (IF)	BD	610923
Rb-anti-BIN1	1:2000 (WB)	Rockland	200-301-E63
Rb-anti-GFP	1:5000 (WB)	GenScript	A01388-40
Rb-anti-GAPDH	1:5000 (WB)	Santa Cruz	25778
<i>Secondary Antibodies</i>			
555-Dk-anti-Gt	1:1000	Invitrogen	A21432
555-Dk-anti-Ms	1:1000	Invitrogen	A31570
555-Dk-anti-Rb	1:1000	Invitrogen	A31572
647-Dk-anti-Gt	1:1000	Invitrogen	A21447
647-Dk-anti-Ms	1:1000	Invitrogen	A31571
647-Dk-anti-Rb	1:1000	Invitrogen	A31573
HRP-Dk-anti-Rb	1:5000	Invitrogen	A16035
<i>Fluorescent Dyes</i>			
DAPI	500 nM	Invitrogen	D3571

555-WGA	5 µg/ml	Invitrogen	W32464
647-WGA	5 µg/ml	Invitrogen	W32466
FM 4-64	100 µg/ml	Invitrogen	T13320

E. Online Movies

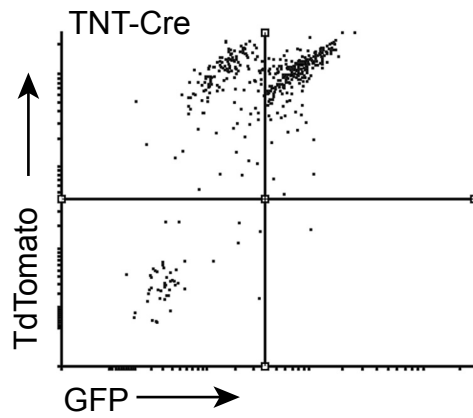
Online Movie I. *In situ* T-tubule imaging in a Jph2_Low heart.

Online Movie II. *In situ* T-tubule imaging in a Jph2_Mid heart.

Online Movie III. *In situ* T-tubule imaging in a Jph2_High heart.

Online Movie IV. *In situ* T-tubule imaging in a RYR2 mosaic mutagenesis heart.

All movies are confocal z-stacks with 2 μm step size that play at 1 stack/second speed. Each movie contains an FM4-64 grey-scale channel to the left and an RGB channel to the right that merges FM4-64 (Magenta) and Cas9GFP (Green) signals. The height of all movie frames is 212 μm .



Online Figure II. Distribution of GFP and tdTomato reporters in *Rosa26*^{Cas9GFP/tdTomato} mice after treatment with AAV9:TNT-Cre. Neonatal mice were treated with AAV:TNT-Cre. Cardiomyocytes were dissociated from adult hearts and analyzed by flow cytometry. As expected, most cardiomyocytes were GFP+ tdTomato+ and there were few GFP+ tdTomato- cells. However, GFP- tdTomato+ cells were noted. This might reflect differential sensitivity of the two different Cre-activated reporters to Cre, and differential sensitivity of GFP or tdTomato expression or stability in cardiomyocytes stressed by dissociation and flow cytometry.

A

The number of predicted off-target sites in mouse genome

Mismatch bp number	Jph2 gRNA1		Jph2 gRNA2	
	exonic	non-exonic	exonic	non-exonic
1	0	0	0	0
2	0	0	0	0
3	0	2	0	6

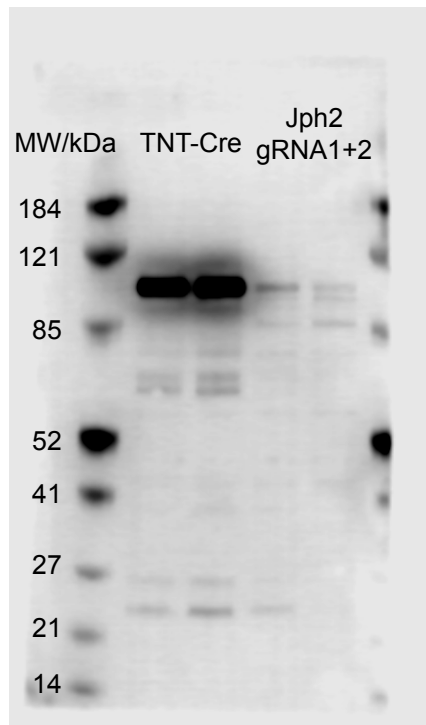
B

		gRNA1 target	PAM
Amp-Seq1 Jph2gRNA1	wildtype	GACTTTGATGATGGCGGGGCGTATTGTGG	GGGCTGGGAAGGGG
	frame-shift deletion	GACTTTGATGATGGCGGGGC-----TGGGAAGGGG	
	frame-shift insertion	GACTTTGATGATGGCGGGGCGTATTGTGGGGGCTGGGAAGGGG	

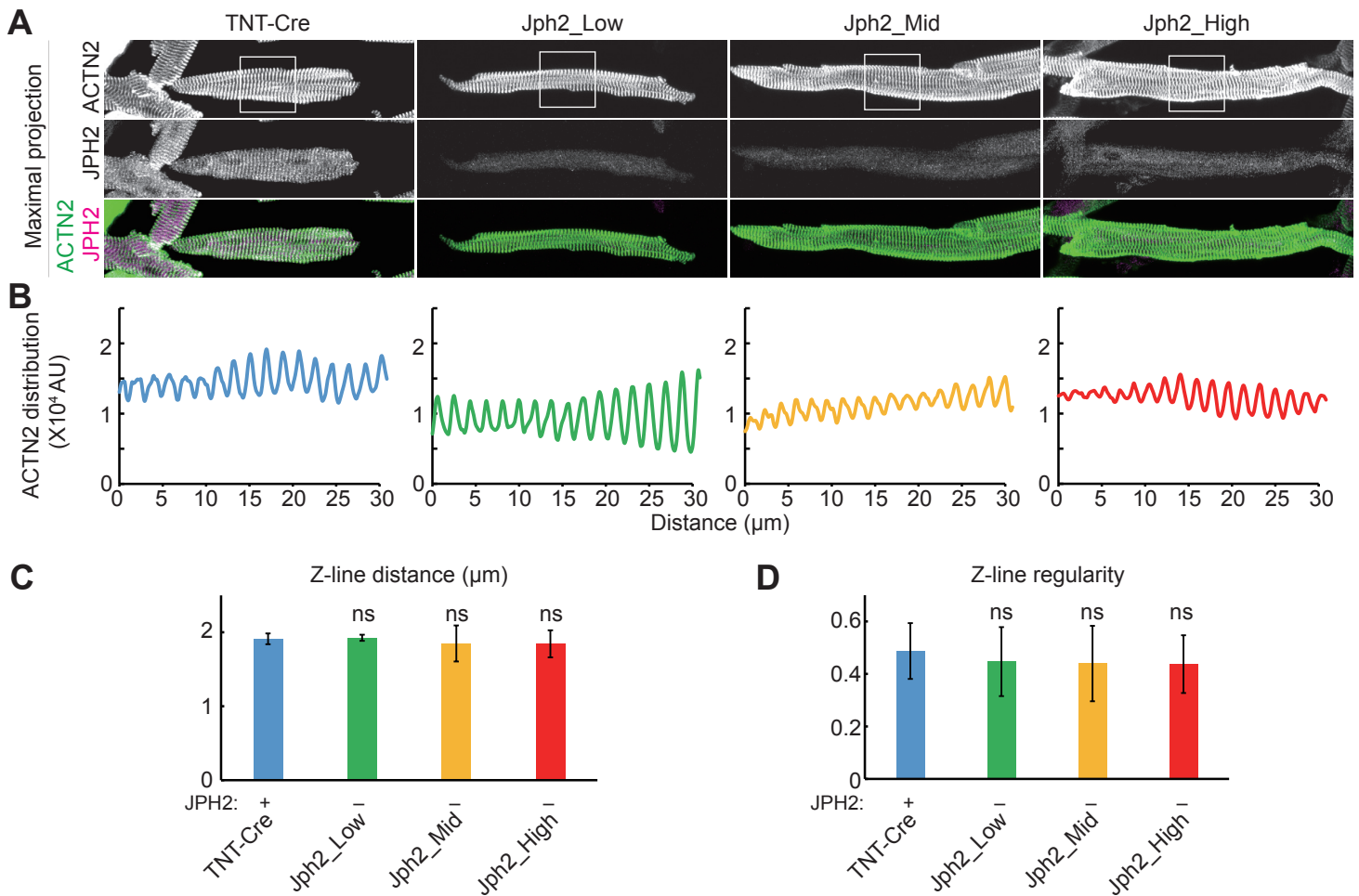
C

		PAM	gRNA2 target
Amp-Seq2 Jph2gRNA2	wildtype	CACAAACAGTGGTGCCAAGTACGAGGGCACTTGGGAAT	AACGGC
	frame-shift deletion	CACAAACAGTGGTGCCAAGT-----GGGCACTTGGGAAT	AACGGC
	frame-shift insertion	CACAAACAGTGGTGCCAAGTAACGAGGGCACTTGGGAAT	AACGGC

Online Figure III. Frame-shift mutations induced by Jph2gRNA-directed Cas9 cleavage followed by NHEJ. (A) The number of predicted off-target sites in the mouse genome for gRNA1 or gRNA2. (B-C) Examples of mutations induced by Jph2gRNA1 or Jph2gRNA2 as determined by amplicon sequencing.

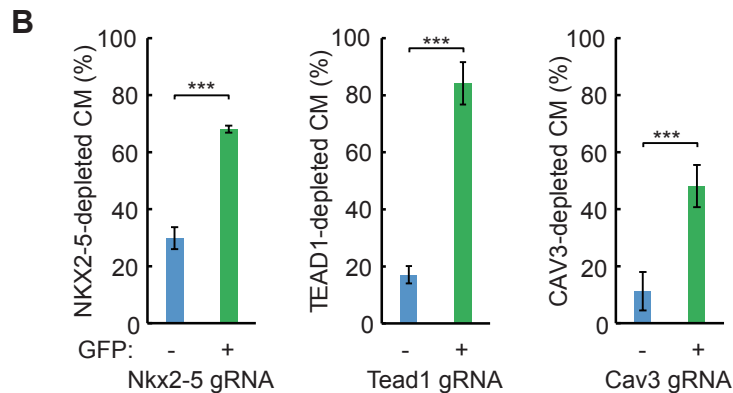
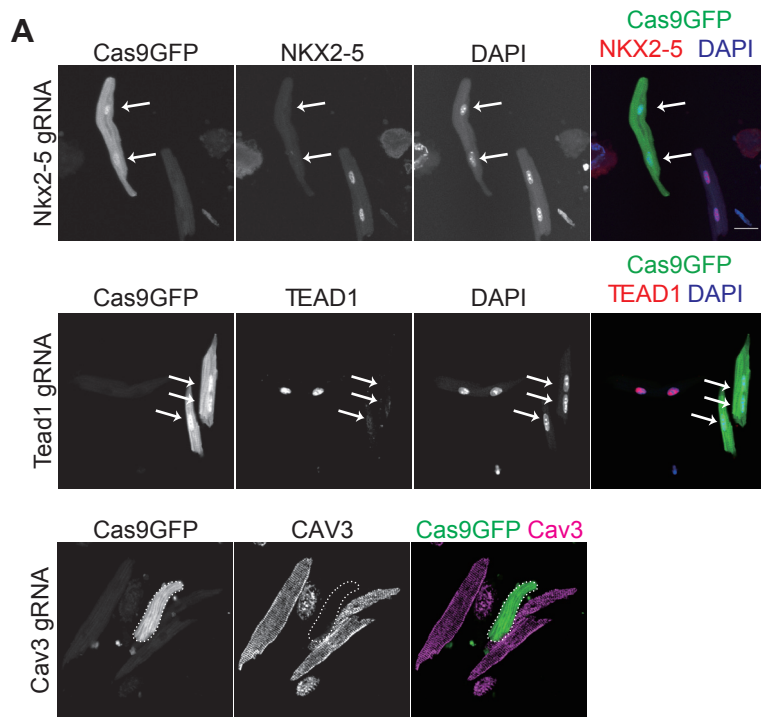


Online Figure IV. JPH2 immunoblot of FACS-sorted GFP+ CMs treated with TNT-Cre or Jph2(gRNA1+2) AAV. This is the full immunoblot of the same gel shown in Fig. 1G, over-exposed to look for minor truncated Jph2 expression products. The major effect of Jph2 gRNAs was reduction of JPH2 level rather than production of a truncated protein.

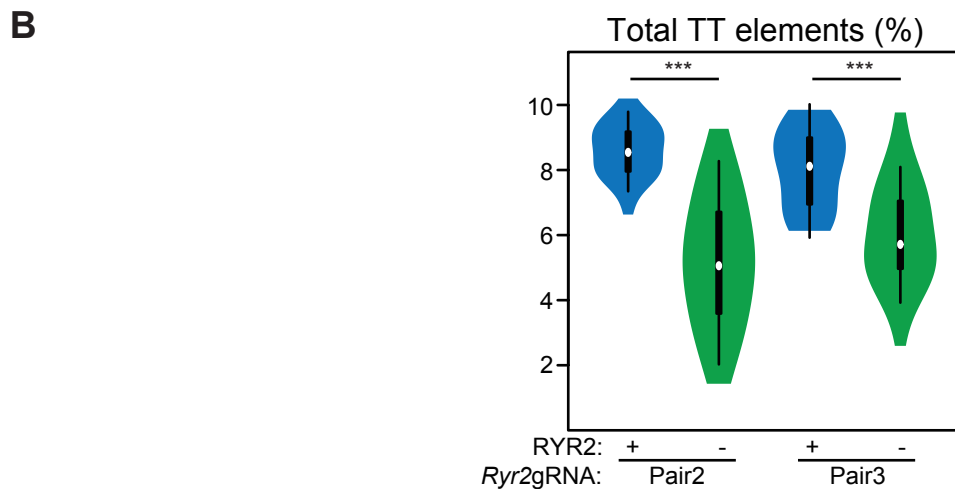
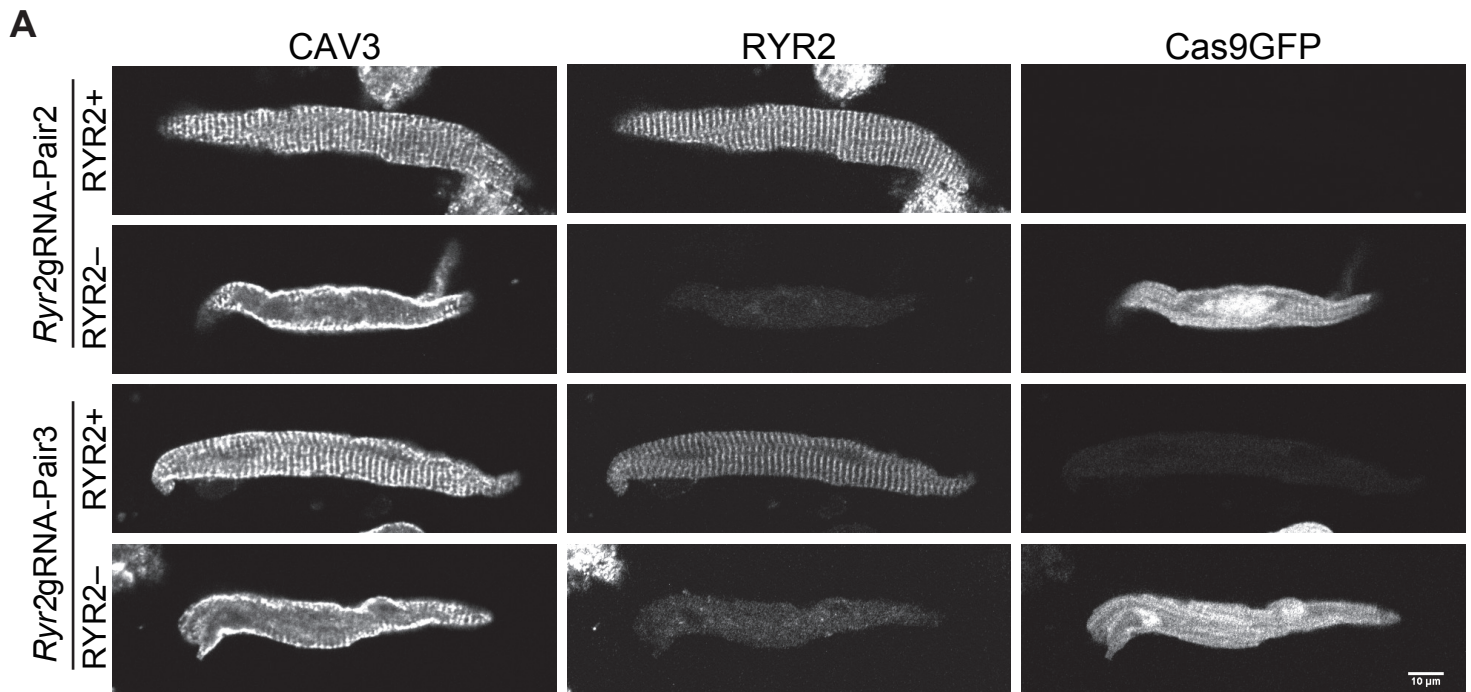


Online Figure V. JPH2 depletion did not cell-autonomously disrupt sarcomere organization.

TNT-Cre or AAV-gRNA(Jph2) were administered at P1 and CMs were isolated at P21. CMs were immunostained for JPH2 and ACTN2. (A) Representative maximal intensity projection images. (B) Longitudinal distribution of ACTN2 fluorescence intensity in a single focal plane of boxed areas in (A). AU, arbitrary unit. (C-D) Quantification of average distance between Z-lines and the regularity of Z-line alignment by AutoTT. Boxed areas in (A) were representative regions that were used to perform this quantification. n=30 CMs isolated from 3 hearts in each group. Student's t-test compared to control (TNT-Cre) cells. ns, not significant. Plots show mean \pm SD.



Online Figure VI. Knockout of NKX2-5, TEAD1 and CAV3 by CASAIV. (A) Immunofluorescence images showing depletion of NKX2-5 (top), TEAD1 (middle) and CAV3 (bottom) in Cas9GFP+ CMs upon mosaic transduction with AAVs that express corresponding gRNAs. Arrows point to nuclear depletion of NKX2-5 and TEAD1. CAV3-depleted cell is delineated by dashed lines. Scale bar, 20 μ m. (B) Quantification of NKX2-5, TEAD1 and CAV3 depletion in GFP- and GFP+ CMs. n=3 hearts. >50 CMs were counted per heart. Student's t-test: *** p <0.001. Plots show mean \pm SD.



Online Figure VII. Mosaic RYR2 depletion using multiple gRNA pairs disrupts T-tubule structure.

(A) RYR2 was depleted using two different pairs of gRNAs. RYR2 and CAV3 were detected by immunostaining, and GFP was detected by endogenous fluorescence. Representative images show that CAV3 T-tubule staining was disrupted by depletion of RYR2 in Cas9GFP+ CMs. Scale bar, 10 micron.

(B) Quantification of CAV3 immunostaining using AutoTT, displayed as violin plots. CMs depleted of RYR2 by either pair of gRNAs had reduced T-tubule organization. Student's t-test: ***, $P < 0.001$.